ACS APPLIED MATERIALS & INTERFACES

Research Article

www.acsami.org

Surface Science and Electrochemical Analysis of Nickel Foams

Michał Grdeń,† Mohammad Alsabet, and Gregory Jerkiewicz*

Department of Chemistry, Queen's University Kingston, Ontario K7L 3N6, Canada

ABSTRACT: Open-pore nickel (Ni) foams are characterized using surface science and electrochemical techniques. A scanning electron microscopy analysis reveals interconnected Ni struts that generate small and large pores of ca. 50 and 500 μm in size, respectively. An X-ray photoelectron spectroscopy (XPS) analysis of the surface-chemical composition of the Ni foams shows that there are oxidized and metallic sections within their surfaces despite being prepared by sintering in an oxidizing atmosphere at a high temperature and being stored in moist air. The ratio of the areas of oxidized and metallic sections is evaluated using XPS data. Chemical etching of the Ni foams results in removal of the native surface oxide/hydroxide without altering the three-dimensional structure; it also increases the roughness (R) of the surfaces of Ni struts giving rise to an increase in the electrochemically active surface area (A_{ecsa}). Thermal treatment of Ni foams in an H_2(g) atmosphere at 500 °C reduces the native surface oxide/hydroxide but does not increase R or A_{ecsa}. Electrochemical behavior of the Ni foams is examined in 0.5 M aqueous KOH solution using cyclic-voltammetry (CV) and electrochemical impedance spectroscopy (EIS). As-received, chemically etched, thermally reduced and electro-oxidized Ni foams generate distinct CV profiles; their features are assigned to oxidized and metallic surface states. The observations made on the basis of XPS measurements are corroborated by the results of CV analyses. The application of CV and XPS or EIS allows in situ determination of A_{ecsa} and the specific surface area (A_s) of the chemically etched and thermally reduced Ni foams. The values of A_s determined on the basis of joint CV and XPS measurements are 227 ± 74 and 149 ± 48 cm^2 g^{-1} for the etched and reduced Ni foams, respectively. The values of A_s determined on the basis of CV, XPS and EIS measurements are 241 ± 80 and 160 ± 23 cm g^{-1} for the etched and reduced Ni foams, respectively

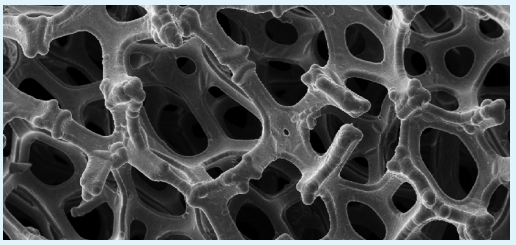

KEYWORDS: *nickel electrode, nickel foam, nickel hydroxide, nickel oxide, chemical etching, real surface area, electrochemically active surface area, X-ray photoelectron spectroscopy, cyclic-voltammetry*

INTRODUCTION

Porous metallic materials possessing high specific surface areas (A_s in cm^2 g^{-1}) and open-pore structures, namely metallic foams, are of importance to electrochemical energy-storing and energy-generating devices, such as batteries, electrochemical supercapacitors and alkaline fuel cells.[1−3] They can be applied either in their native form or can be filled with an active mass; in the latter case they act simultaneously as a current collector and a support matrix.[1,2] Other electrochemical applications of porous materials include flow-through electrolyte electrodes[4−6] and optically transparent electrodes.[3,7] Nickel due to its mechanical strength, inertness, relatively low toxicity and low cost is one of the most important metals and stainless steels are among the most important Ni-containing products. The above-mentioned physical characteristics and corrosion stability in aqueous alkaline solutions make it a suitable material for specialized electrochemical applications. For example, Ni and Ni-based electrodes (e.g., alloys, hydroxides, nickelates)[8−16] are used as electrode materials in water electrolyzers, alkaline fuel cells, electrochemical supercapacitors, electrochromic devices (ECD) and alkaline batteries, both as an active mass (e.g., $Ni(OH)_2$/NiOOH) and as a combined charge carrier and active mass support (e.g., Ni foams, Ni meshes). The preparation of open-pore Ni foams typically involves a polyurethane matrix on which Ni or Ni-containing alloys are deposited. The metallic deposits can be prepared using various methods,[17] but chemical vapor deposition (CVD)[18−22] and electrochemical deposition[1,23,24] are the most important ones. Following the Ni deposition, the polyurethane matrix can either be maintained unchanged, if it does not interfere with an envisaged application,[1] or can be removed by sintering or pyrolysis.[18,19] Nickel foams prepared using CVD or electro-deposition and subsequently sintered at an elevated temperature have a pore size ranging from 450 μm to 3.2 mm.[18] They can be used in statu nascendi or can be modified by depositing noble-metal nanoparticles to accomplished a fine-tailored catalytic property.[25−28] The extended surface area and fine-tuned three-dimensional structure makes them very attractive materials for various electrochemical, catalytic and structural applications. However, the actual determination of their surface area is very difficult and often results in inaccurate results.

In this contribution, we report on the materials science, surface science and electrochemical characterization of commercial Ni foams having an open-pore structure. Because as-received Ni foams are partially passivated, we discuss methods of producing metallic surfaces without introducing any structural changes. As-received, thermally reduced in an H_2(g) atmosphere, chemically etched and electro-oxidized

Received: March 1, 2012
Accepted: May 10, 2012
Published: May 10, 2012

foams are carefully analyzed using surface and materials science, and electrochemical techniques. We examine the three-dimensional structure, surface chemical composition and specific surface area of these foams in relation to their preparation and pretreatment. We present and apply complementary experimental approaches to determine the specific surface area of chemically etched and thermally reduced Ni foams, and show that they yield consistent and accurate results.

EXPERIMENTAL SECTION

Electrochemical Setup and Experiments. Experiments were conducted in an all-glass, three-compartment electrochemical cell. Platinum gauze served as a counter electrode (CE) and a Pt/Pt black reversible hydrogen electrode (RHE) immersed in the same electrolyte solution was used as a reference electrode (RE); H_2(g) of ultrahigh purity (99.999%) and at a pressure of 1.0 atm was passed through the RE compartment; the latter was electrolytically connected to the working electrode compartment through a Luggin capillary. All the potentials (E) applied and reported refer to an RHE scale. Experiments were carried out at room temperature (T = 298 ± 1 K) in 0.5 M aqueous KOH (Sigma-Aldrich) solution that was pre-electrolyzed and then deaerated by bubbling ultrahigh purity N_2(g) (99.999%). All solutions were prepared using deionized water (Millipore) the resistivity of which was 18.2 MΩ cm. The electrochemical experiments were carried out using PAR 263 and PAR 263A potentiostats. Cyclic voltammetry (CV) with various potential limits was employed as the main electrochemical technique. Electrochemical impedance spectroscopy (EIS) was used to measure interfacial capacitance; the experimental setup comprised a PAR 5210 lock-in amplifier coupled with a PAR 263A potentiostat. Data were collected using the PowerSine software and analyzed using the Equivcrt data analysis software. For each type of electrode materials and potentials applied, at least five EIS measurements were carried out. The reported capacitance values were an average of these five measurements. Capacitance experiments were typical EIS measurements in which a frequency (f) spectrum in the 50 kHz to 0.5 Hz range, with a 5 mV root-mean-square AC wave, was recorded at a constant potential. Such obtained spectra were analyzed using the Equivalent Circuit software.[29]

Nickel Foam Characterization. The Ni foams employed in the course of research were several batches of commercial Ni foams (Incofoams) manufactured by former INCO Technical Services Ltd. (later Vale-INCO).[18,19] Scanning electron microscopy (SEM) was employed to examine their three-dimensional structure. The Ni foams of ca. 1.0 mm in thickness were cut into squares (5 ± 0.5 mm in side length) and weighed ca. 0.030 ± 0.005 g each. Because it was impossible to prepare identical Ni samples, each specimen was weighed prior to experiments. Each Ni foam square was attached to a Ni wire (100 μm in diameter) that was sealed in a glass tube. The contribution of the Ni wire to electrochemical signal measured was less than 1%. Such prepared Ni foam materials served as working electrodes (WE).

Treatment of Nickel Foams. Several approaches were employed to treat Ni foams in order to prepare metallic or oxidized surfaces. In the following sections, the Ni foams denoted as "as-received" were subjected only to cleaning that did not alter their chemical composition. The foams were degreased with hot acetone under reflux, rinsed with deionized water and then sonicated in deionized water. The last step involved short sonication of Ni foams in 0.5 M aqueous KOH solution in order to flood the pores. Nickel foams were also either chemically etched or thermally reduced in an H_2(g) atmosphere to produce metallic surfaces. The chemical etching or thermal reduction was preceded by cleaning as described above. Several chemical etching solutions were employed to prepare metallic surfaces but only one yielded the expected result; it is described in detail in Results and Discussion. The thermal reduction was carried out by placing a Ni foam in a quartz tube through which H_2(g) (99.999%) at a pressure of ca. 3.0 atm was passed for 2 h and the temperature was maintained at 500 ± 10 °C. Chemically etched and thermally reduced Ni surfaces are denoted as "etched" and "reduced", respectively. Some Ni foams were subjected to electrochemical passivation that resulted in the formation of β-Ni(OH)$_2$. This was accomplished by repetitive cycling of a Ni foam in the 1.0−1.6 V potential range until a steady-state CV profile was obtained. This approach required ca. 270 cycles and generated a surface that was covered with a thick layer of Ni(OH)$_2$. Such prepared Ni foam surfaces are denoted as "passivated".

Comparative electrochemical measurements were conducted using bulk Ni. A Ni rod of 5.0 mm in diameter (AlfaAesar Puratronic) was sealed in a Teflon sleeve and an electrical contact was made using a threaded stainless steel wire that was screwed into the Ni rod. The Ni rod-wire connection was carefully sealed using a Teflon sleeve (tight fit) and was never exposed to the electrolyte. Prior to each experiment, the Ni rod was mechanically polished with alumina pastes of different grades down to 0.05 μm (Buehler Micropolish Alumina) to obtain a mirror-like surface finish. After the polishing, the electrode was rinsed with deionized water (Millipore) and immediately introduced into the electrochemical cell. In order to avoid any contact with air that could contaminate the electrode surface, the latter was protected during the transfer into the cell with a droplet of deionized water. The surface roughness (R) of such a prepared Ni rod electrode was examined by measuring the charge associated with the formation of α-Ni(OH)$_2$ and was R = 2.10 ± 0.74.[30] The surface roughness is defined by eq 1

$$R = A_{ecsa}/A_g \quad (1)$$

where A_{ecsa} is the electrochemically active surface area and A_g is the geometric surface area. The electrochemically active surface area is the area accessible to electrolyte at which electron transfer takes place and the geometric surface area is a two-dimensional projection of the electrode surface. The Ni rod was also subjected to the same chemical etching as the Ni foam (thermal reduction in an H_2(g) atmosphere was impossible due to the presence of Teflon sleeve). This allowed us to evaluate changes in A_{ecsa} brought about by the chemical etching.

SEM and XPS Characterization. Scanning electron microscopy (SEM) and X-ray photoelectron spectroscopy (XPS) analyses were carried out using a VG Scientific Microlab 310 ultrahigh vacuum (UHV) surface analysis system. SEM micrographs were acquired using a LEO 435VP scanning electron microscope in the Department of Chemistry, Warsaw University. In the XPS measurements, an Al X-ray source was employed and an area of ca. 12 mm^2 was analyzed; an XPS signal from such a large surface area was representative of the entire sample. Since all the Ni samples studies were good electronic conductors, no charge compensation was required. Depth profile analyses were performed using an EX05 argon-ion (VG Scientific Instruments) and Ar(g) of ultrahigh purity Ar (99.999%).

RESULTS AND DISCUSSION

Characterization of Nickel Foams. Figure 1 shows an SEM micrograph of a Ni foam which reveals the existence of interconnected struts that generate small and large open pores, mainly pentagonal in shape and ca. 50 ± 10 μm and 500 ± 100 μm in size, respectively. The large pores dominate the three-dimensional structure and the small pores are observed mostly in the regions where struts interconnect; not all strut interconnections create small pores. Paserin et al. showed that the interior of struts is hollow.[18,19] However, the hollow internal structure does not affect the exterior morphology and the struts are found to be mostly compact and fairly uniform, and their surfaces do not show any openings or voids.

Chemical Etching. Nickel foams were chemically etched to: (i) generate a metallic surface by removing a native oxide/hydroxide layer that developed on the foam surface during sintering[18,19] and prolonged exposure to moist air;[31−34] (ii) increase the surface roughness of Ni foams (rough surfaces are

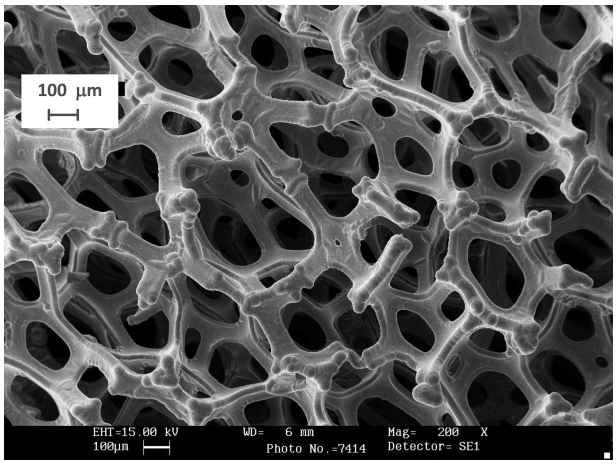

Figure 1. SEM micrograph of a Ni foam obtained at a magnification 200×.

known to be more active than smooth ones); and (iii) modify the electrocatalytic activity of Ni foams (a metallic surface has different electrocatalytic properties than an oxidized one). Table 1 presents the chemical compositions of four etching solutions and the description of experimental procedure employed. The etching solution 4 was found to be unsuitable for treating Ni foams because it resulted in their total dissolution within less than 1 min. On the other hand, chemical etching in the etching solutions 1 through 3 maintained the integrity of Ni foams. Consequently, we performed CV measurements using Ni foams treated in the etching solutions 1 through 3 with the objective of obtaining a profile characteristic of a metallic Ni electrode. The Ni foams treated in the etching solutions 2 and 3 generated CV profiles (not shown) that did not resemble at all that expected for metallic Ni. However, Ni foams treated in the etching solution 1 generated a CV profile characteristic of a metallic Ni surface (see next section), and, consequently, this etching solution was employed in further research.

Table 1. Composition of etching solutions and procedures employed to chemically etch Ni materials.

etching solution	etching solution composition	etching procedure	literature source
1	30 cm^3 conc. HNO_3	T = 18−19 °C	52, 62−64
	10 cm^3 conc. H_2SO_4	etching time = 2 min	
	10 cm^3 conc. H_3PO_4	no stirring	
	50 cm^3 glacial CH_3COOH		
2	25 cm^3 conc. HNO_3	T = 18−19 °C	65
	10 cm^3 H_2SO_4	etching time ≤ 10 min	
	25 cm^3 glacial CH_3COOH	no stirring	
	40 cm^3 H_2O		
3	75 g L^{-1} $KMnO_4$	T = 75−100 °C	65
	75 g L^{-1} Na_2CO_3	etching time ≤ 10 min	
	H_2O to 1 L	no stirring	
4	120 cm^3 conc. H_2SO_4	T = 85 °C	65
	90 g L^{-1} KNO_3	etching time ≤ 2 min	
	90 g L^{-1} NaCl	stirring	
	H_2O to 1 L		

Because chemical etching resulted in an irreversible loss of Ni, it became necessary to examine changes in the mass of Ni foams as a function of etching duration. This was done by applying different etching times in the 35−180 s range and examining the percentage of mass loss as compared to the mass of Ni foam prior to chemical etching (Figure 2). The results demonstrate that there is a linear relationship between the percentage of mass loss and the etching time, for etching times up to 180 s. They also show that the etching for 30 − 40 s results in a 10% mass loss while the etching for 180 s results in a 26% mass loss. It is important to add that mass losses are not only due to dissolution of Ni but possibly also due to detachment of small sections of foams as a result of etching-induced breakup of the structure in areas where struts become thin.

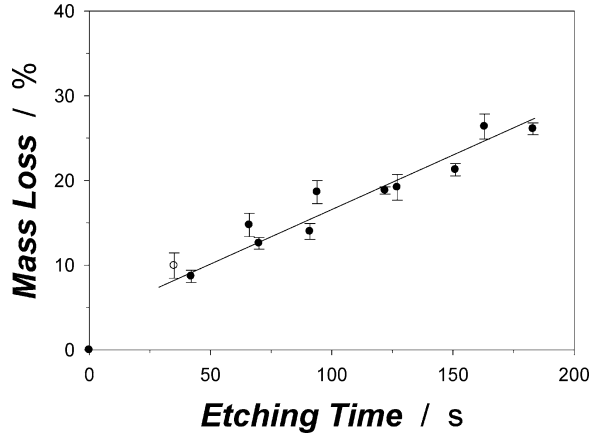

Figure 2. Relationship between the percentage of mass loss and the etching time for Ni foams treated in the etching solution 1. The etching solution composition and the etching procedure are presented in Table 1.

Scanning Electron Microscopy and X-ray Photoelectron Spectroscopy Characterization of Ni Foams. Figure 3 presents three SEM micrographs for: (i) the "as-received" Ni foam (A); (ii) the "etched" Ni foam for 120 s (B); and (iii) the "etched" Ni foam for 180 s (C). The image A reveals a compact structure with well-defined grains and narrow grain boundaries. The image B demonstrates that chemical etching for 120 s increases the surface roughness within local surface regions but without altering the three-dimensional structure. The image C reveals that chemical etching for 180 s damages the three-dimensional structure by developing small and large voids, which expose the internal foam structure. The enhancement of surface features (image B) and structural changes (image C) can be related to the mass losses reported in Figure 2.

We conducted X-ray photoelectron spectroscopy (XPS) measurements in order to examine the surface chemical composition of untreated and pretreated Ni foams. Figure 4 presents XPS spectra of the Ni($2p_{3/2}$) and Ni($2p_{1/2}$) bands and their satellites for the following Ni samples: (i) the "as-received" Ni foam (A); (ii) the "passivated" Ni foam by cycling 270 times in the 1.0 − 1.6 V range (B); (iii) the "etched" Ni foam for 70 s (C); (iv) the "etched" Ni foam for 120 s (D); (v) the "reduced" Ni foam (E); and (vi) the Ni foil sputtered with Ar^+ ions under ultrahigh vacuum (UHV) conditions (F); the

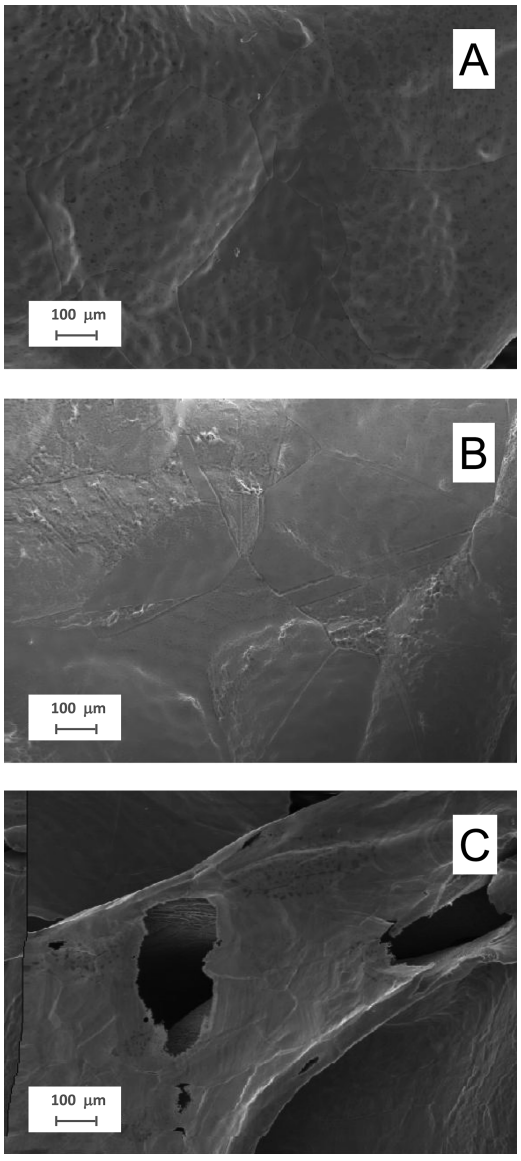

Figure 3. SEM micrographs at a magnification 1000× for (A) the "as-received" Ni foam, (B) the "etched" Ni foam treated in the etching solution 1 for 120 s, and (C) the "etched" Ni foam treated in the etching solution 1 for 180 s. The etching solution composition and the etching procedure are presented in Table 1.

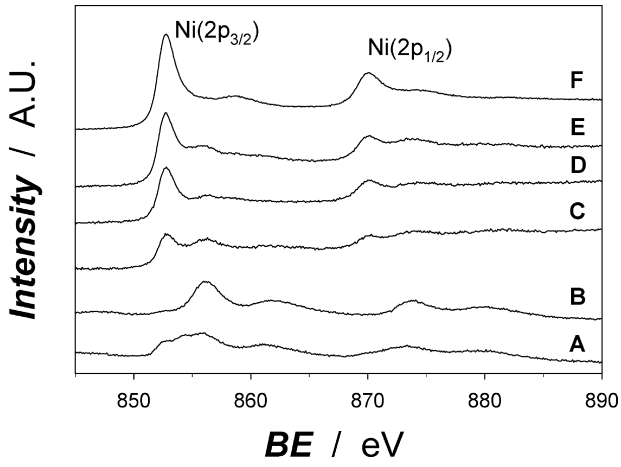

Figure 4. XPS spectra of the Ni($2p_{3/2}$) and Ni($2p_{1/2}$) bands and their satellites for: (A) the "as-received" Ni foam, (B) the "passivated" Ni foam by cycling 270 times in the 1.0−1.6 V potential range, (C) the "etched" Ni foam for an etching time of 70 s, (D) the "etched" Ni foam for an etching time of 120 s, (E) the "reduced" Ni foam, and (F) the Ni foil sputtered with Ar^+ ions under ultrahigh vacuum (UHV) conditions.

sputtering produced in situ an oxide-free Ni surface that served as a reference. XPS spectra for two etching times are presented in order to examine the impact of the etching duration on the surface chemical composition of Ni foams. We observe that the XPS spectra for Ni foams generate less-sharp XPS peaks than in the case of low roughness, bulk Ni because the electrons entering the hemispherical electron energy analyzer have a broad range of takeoff angles. This behavior is characteristic of rough and porous materials, and nanoparticles. Detailed discussion and interpretation of Ni XPS spectra, such as the number of peaks produced by deconvolution, is well-documented and can be found elsewhere.[35−42] Here, we focus our analysis only on the Ni($2p_{3/2}$) peak and its satellite, which are easily distinguishable and allow examination of the oxidation state of Ni in the surface region of Ni foams. According to the literature, the binding energy (BE) of the Ni($2p_{3/2}$) peak is 852.7 eV for Ni(0), 854 eV for Ni(2+) in the form of NiO, and 856 eV for Ni(2+) in the form of $Ni(OH)_2$. The binding energy of the satellite peak is 858 eV in the case of Ni(0), 860.7 eV in the case of NiO, and 861.2 eV in the case of $Ni(OH)_2$.[36,38,43] The "as-received" Ni foam (A) reveals a weak peak for Ni(0) and a prevailing peak for Ni(2+) as well as their satellites. The "passivated" Ni foam (B) shows a well-defined peak at 856 eV characteristic of Ni(2+) and its satellite. The lack of peak at 852.7 eV characteristic of Ni(0) indicates that the entire "passivated" Ni foam surface is oxidized, as expected. It is interesting to observe that the degree of passivation of the "as-received" Ni foam is significantly smaller than that of the "passivated" one. The "etched" Ni foams for 70 and 120 s etching times (C and D, respectively) display two peaks at 852.7 and 856 eV, respectively, and their satellites; they point to the presence of Ni(0) and Ni(2+). The increase in etching time from 70 to 120 s enhances the intensity of the Ni(0) peak and decreases the intensity of the Ni(2+) peak. The "reduced" Ni foam (E) shows a well-defined peak at 852.7 eV and a small one at 856 eV, and their satellites; they indicate that a majority of the surface is reduced to metallic Ni but there are still some oxidized sections. Finally, the Ni foil sputtered with Ar^+ ions reveals a well-defined peak at 852.7 eV and its satellite indicating that the Ni foam surface is metallic; there are no spectral features that could be assigned to Ni(2+). An analysis of the XPS spectra shows that the degree of oxidation of the "as-received" Ni foam is greater than that of the "etched" or "reduced" Ni foams and lower than that of the "passivated" Ni foam. It also shows that the XPS spectra for the "etched" and "reduced" Ni foams are very similar, thus indicating that these two procedures generated surfaces that possessed both metallic and oxidized sections, with the metallic state being prevalent. It is important to observe that an XPS analysis of the "etched" Ni foam always reveals the presence of a small peak and its satellite characteristic of Ni(2+). At this stage, we assign this behavior to partial oxidation of an active Ni foam surface by molecular oxygen dissolved in the deionized water used for sample rinsing.

General Electrochemical Behavior of Ni Foams. Figure 5 shows CV profiles in 0.5 M aqueous KOH solution recorded

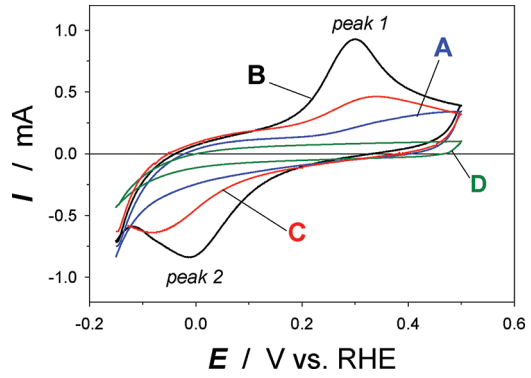

Figure 5. CV profiles in 0.5 M aqueous KOH solution obtained at T = 298 K and s = 100 mV s^{-1} in the $-0.15 \leq E \leq 0.50$ V potential range for (A) the "as-received" Ni foam, (B) the "etched" Ni foam for 2 min, (C) the "reduced" Ni foam, and (D) the "passivated" Ni foam.

at T = 298 K and a scan rate of s = 100 mV s^{-1} in the $-0.15 \leq E \leq 0.50$ V potential range for: (i) the "as-received" Ni foam (A); (ii) the "etched" Ni foam for 2 min (B); (iii) the "reduced" Ni foam (C); and (iv) the "passivated" Ni foam (D).

The CV profiles reveal an anodic peak in the 0.2−0.4 V potential range (peak 1) that is due to oxidation of Ni(0) to Ni(2+) in the form α-$Ni(OH)_2$ and a cathodic peak in the −0.12 to 0.12 V potential range (peak 2) that is due to reduction of α-$Ni(OH)_2$ to Ni(0).[44−50] The peak potentials of these features strongly depends on the surface state and any pretreatment applied. The peaks 1 and 2 are observed only in the case of metallic Ni, thus a Ni electrode surface that is free of any β-$Ni(OH)_2$ or β-NiOOH. Therefore, the presence or absence of the peaks 1 and 2 in CV profiles for Ni materials is indicative of the chemical state of their surfaces (metallic vs oxidized). A comparison of the CV profiles leads to the following observations: (i) the "as-received" Ni foam is almost completely oxidized as confirmed by XPS measurements (Figure 4, spectrum A); a CV profile in the −0.15 to 0.60 V potential range reveals the presence of a small anodic peak in the 0.35 to 0.55 V potential range that is due to metallic Ni oxidation (results not shown); (ii) the "passivated" Ni foam does not reveal the peaks 1 and 2 because its entire surface is covered with a thick layer of electrochemically irreducible β-$Ni(OH)_2$; this observation is corroborated by XPS data (Figure 4, spectrum B); (iii) the "etched" Ni foam reveals well-defined peaks 1 and 2 at 0.30 and −0.01 V, respectively; their presence demonstrates that the Ni foam surface is mostly metallic in nature; this observation is supported by XPS measurements (Figure 4, spectrum D); the increase in peak currents can be attributed to an increase of the surface area brought about by the etching; this observation is supported by SEM data (Figure 3, image B); (iv) the "reduced" Ni foam reveals the peaks 1 and 2 at 0.34 and −0.08 V, respectively; their presence shows that the surface has a significant percentage of metallic character, in agreement with XPS results (Figure 4, spectrum E); and (v) the difference in potentials of the peaks 1 and 2 increases from 0.31 for the "etched" Ni foam to 0.42 V for the "reduced" Ni foam showing that the formation and reduction of α-$Ni(OH)_2$ depends on the surface treatment. It is interesting to observe that the chemical etching generates an oxide-free Ni foam surface whose A_{ecsa} is ca. twice larger than that of the "reduced" Ni foam. This observation suggests that the chemical etching either significantly increases the external surface of Ni foam being in contact with the electrolyte or that the chemical etching creates openings in the Ni foam skin effectively exposing the internal structure. Although our SEM data for a Ni foam etched for 120 s do not reveal the presence of openings in the Ni foam external structure, the existence of such an effect especially in a localized area cannot be entirely excluded.

For a comparative analysis, Figure 6 shows CV profiles in 0.5 M aqueous KOH solution recorded at T = 298 K and s = 100 mV s^{-1} in the $-0.15 \leq E \leq 0.50$ V range for "etched" and "polished" Ni rods. Both CV profiles show clearly defined peaks 1 and 2, but their currents are larger in the case of the "etched" Ni rod. The peaks 1 and 2 are at 0.30 and 0.03 V in the case of "etched" Ni rod and at 0.32 and −0.04 V in the case of "polished" Ni rod; the respective differences in peak potentials are 0.27 and 0.36 V. These results support the observation that the formation and reduction of α-$Ni(OH)_2$ depends on the surface treatment, as noticed for the "etched" Ni foam.

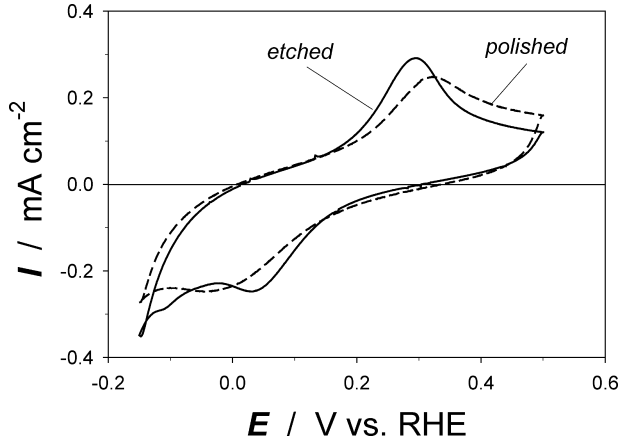

Figure 6. CV profiles in 0.5 M aqueous KOH recorded at T = 298 K and s = 100 mV s^{-1} in the $-0.15 \leq E \leq 0.50$ V potential range for the "etched" and "polished" Ni rods.

Determination of the Electrochemically Active and Specific Surface Areas through Cyclic-Voltammetry Measurements. Porous catalytic materials are very important because they offer an extensive use of the material mass, while maintaining an extended three-dimensional structure and a large surface area. Assessment of the utilization of catalytic materials requires that their total surface areas be known, otherwise qualitative and quantitative comparison of different catalytic materials is impossible. In electrochemistry and electrocatalysis, it is important to differentiate between the real (total) surface area (A_r) and the electrochemically active surface area (A_{ecsa}). The real surface area is the area of the interface separating two phases, typically a solid and a liquid; the electrochemically active surface area of a solid/liquid interphase is the part of the interface or fraction of A_r where electron transfer can take place. The electrochemically active surface area never exceeds the real one ($A_{ecsa} \leq A_r$) and can even be significantly smaller. There are two most common reasons for this behavior: one is physical blocking of a fraction of the real surface to create an electrical contact with a catalytically inactive support (e.g., Pt nanoparticles on a carbon support) and the other is physical blocking of the real surface by nonconducting materials (e.g., insulating polymeric materials, trapped gas bubbles). In the case of Ni materials possessing an extended surface, it is possible to use the charge of formation of α-$Ni(OH)_2$ to determine A_{ecsa} by accepting that

the charge density associated with the formation of one monolayer (ML) of α-Ni(OH)$_2$ is $q_{Ni(OH)2}$ = 514 μC cm^{-2}.[30] However, this approach requires that the entire Ni surface be in a metallic state prior to the α-Ni(OH)$_2$ formation and that the ohmic resistance of the electrolyte solution be small otherwise a significant IR drop might prevent the Ni electrode surface from undergoing electro-oxidation because the locally experienced potential might significantly differ from the applied one.

Our XPS and CV results demonstrate that Ni materials employed in the course of our research (e.g., foams and rods) were never completely metallic due to partial oxidation during the sample handling that exposed freshly etched Ni materials to deionized water containing dissolved molecular oxygen. Because the determination of A_{ecsa} through the α-Ni(OH)$_2$ formation does not take into account the Ni surface already covered with a layer of electrochemically irreducible oxide (e.g., β-Ni(OH)$_2$ or β-NiOOH), the XPS results can be used to calculate a correction factor (f_{corr}). This is accomplished by evaluating the areas under the Ni(2+) and Ni(0) peaks of the Ni(2p$_{3/2}$) band and their satellites ($A_{Ni(2+)}$ and $A_{Ni(0)}$), and then determining their ratio ($r = A_{Ni(2+)}/A_{Ni(0)}$); accordingly f_{corr} = 1 + r. The values of $A_{Ni(2+)}$ and $A_{Ni(0)}$ include the respective sensitivity factors, so that the ratio of areas under XPS peaks corresponds to the ratio of surface areas of actually oxidized and metallic section of Ni foams. The surface area where α-Ni(OH)$_2$ develops as examined by CV (A_{CV}) is evaluated by integrating the part of CV profile corresponding to this surface reaction. Such an evaluated value of A_{CV} can be related to A_{ecsa}, r, and f_{corr} through eq 2:

$$A_{ecsa} = A_{CV}\ f_{corr} = A_{CV}(1 + r) \quad (2)$$

We evaluated A_{CV} for the "etched" and "reduced" Ni foams by determining an average of the anodic (formation) and cathodic (reduction) charges ($\bar{Q}_{Ni(OH)2}$ = 1/2(Q_{AN} + Q_{CATH})) and by dividing it by $q_{Ni(OH)2}$ = 514 μC cm^{-2}. Such determined values of A_{CV} for the "etched" and "reduced" Ni foams are 5.45 ± 0.27 and 2.79 ± 0.14 cm^2, respectively.

Figure 7 presents XPS spectra (black lines) of the Ni(2p$_{3/2}$) and Ni(2p$_{1/2}$) bands and their satellites for the "etched" (A) and "reduced" (B) Ni foams. The blue lines show four peaks generated by deconvoluting the XPS spectra of the Ni(2p$_{3/2}$) band and its satellite into four peaks, two peaks representing Ni(0) and two peaks representing Ni(2+). The assignment of peaks and their binding energies (BE) is as follows: Ni(0) and its satellite are at BE = 852.7 and 857−858 eV, respectively; Ni(2+) and its satellite are at BE = 855−856 and 861 eV, respectively. The red lines show XPS spectra generated by convoluting the four peaks shown as blue lines. The good agreement between the experimental results (black lines) and the spectra (red lines) generated by combining the four peaks (blue lines) validates the XPS peak deconvolution.

Evaluation of the areas under the Ni(2+) and Ni(0) peaks of the Ni(2p$_{3/2}$) band and its satellite allowed us to determine the values of r for the "etched" and "reduced" Ni foams that are 0.25 ± 0.01 and 0.60 ± 0.03, respectively; the corresponding values of f_{corr} are 1.25 ± 0.062 and 1.60 ± 0.080. Knowledge of f_{corr} allows evaluation of the values of A_{ecsa} for the "etched" and "reduced" Ni foams that are 6.81 ± 0.68 and 4.47 ± 0.45 cm^2, respectively. Because the Ni foams were free of any impurities or particulates that could physically block parts of their surfaces, the experimentally determined A_{ecsa} equals A_r. Finally, we can determine the values of specific surface areas (A_s) for the "etched" and "reduced" Ni foams that are 227 ± 74 and 149 ± 48 cm^2 g^{-1}, respectively; they refer to one gram of Ni foam prior to chemical etching or electrochemical pretreatment. It is important to elaborate on the origin of the large uncertainties that are 30 and 40%, respectively. The overall uncertainty is the sum of several experimental uncertainties related to: (i) the preparation of square-shaped Ni foam samples − it is impossible to prepare two Ni foam squares having exactly the same external dimensions; (ii) the weight of Ni foam samples − different batches of Ni foams can have different thicknesses and densities; (iii) the change in the sample weight brought about by chemical etching or electrochemical passivation − the loss of mass brought about by chemical etching is not always the same because different batches of Ni foams can dissolve at different rates; (iv) the determination of $\bar{Q}_{Ni(OH)2}$ − the cathodic component of CV profile due to the reduction of Ni(OH)$_2$ overlaps the region of HER giving rise to experimental uncertainty; and (v) the determination of r. Our analysis of the sources of experimental uncertainty suggests that its magnitude need not be as large as 30−40%. Specifically, in the case of bulk Ni materials (wires, sheets, rods) the experimental uncertainty could be in the 3−5% range, whereas in the case of Ni materials possessing an extended surface area (foams, fine powders, nanoparticles), it could be as large as 30−50%.

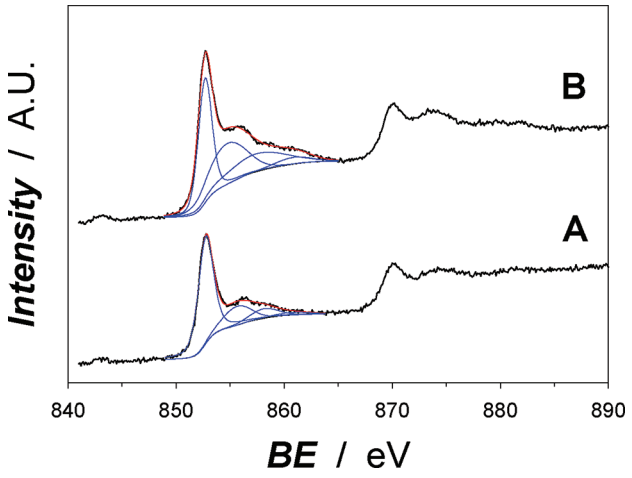

Figure 7. XPS spectra (black lines) of the Ni(2p$_{3/2}$) and Ni(2p$_{1/2}$) bands and their satellites for the (A) "etched" and (B) "reduced" Ni foams. The blue lines show four peaks generated by deconvoluting the spectra of the Ni(2p$_{3/2}$) band and its satellite; two peaks represent Ni(0) and two peaks represent Ni(2+). The assignment of peaks and their binding energies (BE) is as follows: Ni(0) and its satellite are at BE = 852.7 and 857−858 eV, respectively; Ni(2+) and its satellite are at *BE* = 855−856 and 861 eV, respectively. The red line shows XPS spectra generated by convoluting the four peaks shown as blue lines.

Improvement in the Determination of Electrochemically Active and Specific Surface Areas through Interfacial Capacitance Measurements. Measurements of the interfacial capacitance offer an improvement in determining A_{ecsa}. In the case of a surface having metallic and oxidized sections, the total interfacial capacitance (C_{tot}) is a sum of the metal/electrolyte and oxide/electrolyte capacitances (C_m and C_{ox}) connected in parallel as expressed by eq 3:

$$C_{tot} = C_m + C_{ox} \quad (3)$$

The total capacitance can be related to the surface areas of the metallic and oxidized sections of the material (A_m and A_{ox}) through eq 4

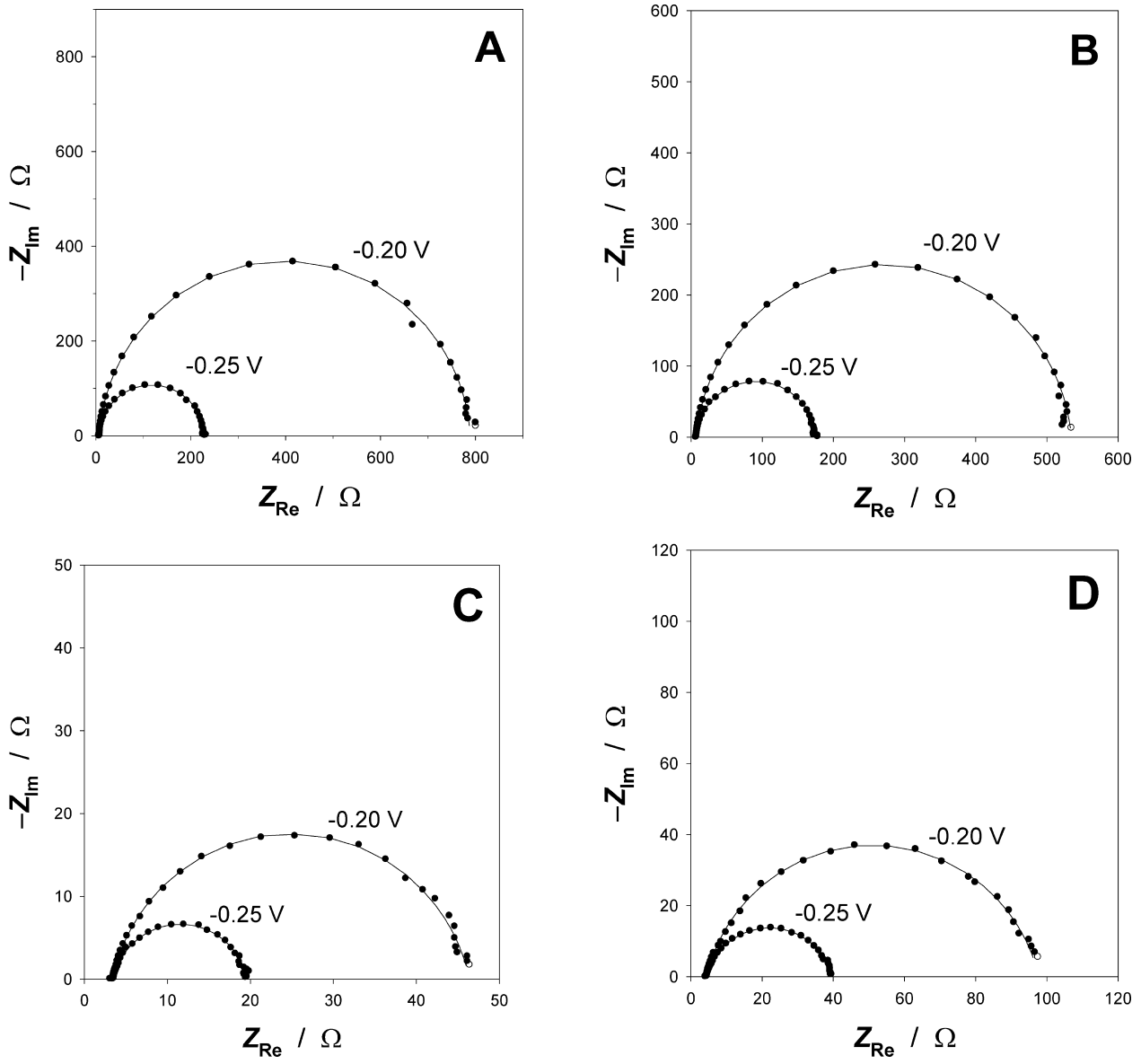

Figure 8. Nyquist plots, Z_{Im} vs Z_{Re}, at $E = -0.20$ and -0.25 V in 0.5 M aqueous KOH solution at $T = 298$ K for (A) the "polished" Ni rod, (B) the "etched" Ni rod, (C) the "etched" Ni foam, and (D) the "reduced" Ni foam. Points represent experimental results and solid lines represent fits obtained using the equivalent circuit shown in Figure 9.

$$C_{tot} = A_m c_{m,s} + A_{ox} c_{ox,s} \quad (4)$$

where $c_{m,s}$ and $c_{ox,s}$ are the specific capacitances (capacitance per unit of the surface area) of the metallic and oxidized sections of material. In the case of pure metallic surfaces $A_{ox} = 0$ and $C_{tot} = C_m$; in the case of fully oxidized surfaces $A_m = 0$ and $C_{tot} = C_{ox}$. Electrochemical impedance spectroscopy measurements allow the determination of C_{tot} and then the evaluation of A_{ecsa}, provided that: (a) $c_{m,s}$ and $c_{ox,s}$ are known, and (b) the electrode surface is either completely metallic or fully oxidized. In the case of electrode surfaces having both metallic and oxidized sections, the same approach can be used to determine A_{ecsa} provided that the ratio of the oxidized and metallic surface areas ($r = A_{ox}/A_m$) is known or can be determined using an alternative approach. Subsequently, A_{ecsa} can be calculated using eq 5:

$$A_{ecsa} = A_m(1 + r) \quad (5)$$

It is apparent that in the case of Ni foams $A_{CV} = A_m$, because α-$Ni(OH)_2$ can develop only on a metallic section of a Ni foam and, consequently, eqs 5 and 2 are equivalent and refer to the same value of A_{ecsa}. The value of $c_{m,s}$ for metallic and adsorbate-free Ni in the $-0.25 \leq E \leq -0.20$ V range and in alkaline electrolyte solutions is $c_{m,s} = 20$ μF cm^{-2},[52−54] but the value of $c_{ox,s}$ is unknown. Capacitance measurements show that oxidation of metallic electrodes often decreases C_{tot} indicating that $c_{ox,s} < c_{m,s}$. Thus, any evaluation of A_{ecsa} that neglects the capacitive contribution from an oxidized electrode section results in an inaccurate result. Therefore, knowledge of $c_{ox,s}$ is absolutely necessary in accurate evaluation of A_{ecsa}.

In order to eliminate any uncertainty in the determination of C_{tot} originating from a surface oxide, EIS measurements were conducted at $E = -0.20$ and -0.25 V, thus in a potential range where only the hydrogen evolution reaction (HER) takes place. We focus our analysis on the determination of C_{tot} because kinetic and mechanistic studies of HER are outside the scope of

this research. Figure 8 shows representative examples of Nyquist plots, Z_{Im} vs Z_{Re} where Z_{Im} and Z_{Re} are imaginary and real parts of impedance, at $E = -0.20$ and -0.25 V in 0.5 M aqueous KOH solution at $T = 298$ K for the "polished" Ni rod (A), the "etched" Ni rod (B), the "etched" Ni foam (C), and the "reduced" Ni foam (D).

All impedance spectra reveal only one semicircle and agree with published data for HER on Ni electrodes.[53,55,56] An analysis of the EIS spectra leads to the observation that a single capacitor cannot represent C_{tot} and a constant phase element (CPE) has to be applied to accomplish the best fit.[57,58] The CPE is defined by eq 6:

$$\mathrm{CPE} = Y_o(i\omega)^n \tag{6}$$

where Y_o is a pre-exponential factor, i is the imaginary unit, $\omega = 2\pi f$ with f being the frequency of the EIS signal, and n is an exponential factor ($n = 1$ for pure capacitor).[58] In a typical equivalent circuit used to model HER in alkaline media, *CPE* is connected in series with an ohmic resistance (R_Ω). The Faradaic branch of equivalent circuit used for an analysis of HER on Ni electrodes contains a charge transfer resistance (R_{ct}) connected in series with a subcircuit containing an additional charge transfer resistance (R_{ct}') and a pseudocapacitance (C_ϕ) connected in parallel. The pseudocapacitance is due to overpotential-deposited hydrogen (H_{OPD}) that acts as an intermediate of HER.[53,56] However, under our experimental conditions (a low frequency limit of 0.5 Hz and a low value of R_{ct} for $E \leq -0.2$ V) the determination of C_ϕ with an acceptable uncertainty is very difficult, if possible at all. Moreover, at such negative potential values, the surface coverage of H_{OPD} reaches a limiting value[53,59] and, as a result, the contribution from C_ϕ may be assumed to be negligible. Thus, the Faradaic branch of the equivalent circuit can be reduced to only one charge transfer resistance (R_{ct}) and yield a simplified equivalent circuit (Figure 9) that we use to model our results. The fits of EIS spectra are shown as solid lines in Figure 8. In Table 2, we report values of R_Ω, Y_o, n and R_{ct} for $E = -0.20$ and -0.25 V determined by fitting the EIS spectra. According to Brug et al.,[57] the values of R_Ω, Y_o, n, and R_{ct} can be used to calculate C_{tot} using eq 7:

$$C_{tot} = [Y_o(R_\Omega^{-1} + R_{ct}^{-1})^{n-1}]^{1/n} \tag{7}$$

In Table 2, we report C_{tot} values for the "polished" Ni rod, the "etched" Ni rod, the "etched" Ni foam, and the "reduced" Ni foam; we notice that in all cases very similar values of C_{tot} are obtained for $E = -0.20$ and -0.25 V. These C_{tot} values can be used to determine A_{ecsa} of metallic Ni materials by using eq 8 because in this case $C_{tot} = C_m$:

$$A_{ecsa} = \frac{C_m}{c_{m,s}} \tag{8}$$

We used this formula and an average of the experimentally determined values of C_{tot} at $E = -0.20$ and -0.25 V (Table 2) to calculate A_{ecsa} of the "polished" and "reduced" Ni rods and found that A_{ecsa} equals 0.370 ± 0.080 cm^2 and 0.530 ± 0.120 cm^2, respectively. However, this approach may not be applied to determine A_{ecsa} of the Ni foams because XPS measurements (Figure 4) show that the "etched" and "reduced" Ni foams had a non-negligible quantity of surface oxide/hydroxide. Thus, it became necessary first to determine $c_{ox,s}$ and then to calculate A_{ecsa}.

The determination of $c_{ox,s}$ involved the following steps: (i) preparation of an unoxidized Ni foam surface; (ii) determination of its A_{ecsa} through CV measurements; (iii) complete oxidation of the Ni foam surface; and (iv) evaluation of C_{tot} through EIS measurements, which in this case equals C_{ox}. Because chemical etching and thermal reduction produce surfaces that are chemically similar but have significantly different surface areas, we prepared unoxidized Ni foams using these two procedures and then passivated them by repetitive cycling in the 1.0 − 1.6 V potential range until a thick layer of $Ni(OH)_2$ developed (see Experimental Section). These two Ni foams are referred to as "etched-passivated" and "reduced-passivated", respectively. In the analysis that follows, we use the A_{ecsa} values that were determined through combined CV and XPS measurements and equal 6.81 ± 0.68 and 4.47 ± 0.45 cm^2, respectively. Figure 10 presents EIS spectra for the "etched-passivated" (A) and "reduced-passivated" (B) Ni foams at $E = -0.225$ V. We fitted the EIS spectra using the same equivalent circuit shown in Figure 9 and determined the values of R_Ω, Y_o, n and R_{ct}, and calculated C_{tot} using eq 7; in this case $C_{tot} = C_{ox}$. Such determined C_{ox} values were 54.2 ± 8.0 and 35.9 ± 6.0 μF for the "etched-passivated" and "reduced-passivated" Ni foams,

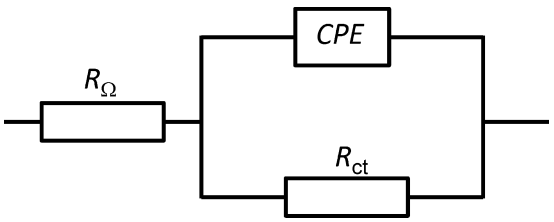

Figure 9. Equivalent circuit used for fitting the EIS spectra presented as points in Figures 8 and 10.

Table 2. Values of R_Ω, Y_o, n, R_{ct}, and C_{tot} at $E = -0.20$ and -0.25 V Determined by Fitting the EIS Spectra.

parameter at given potential	polished Ni rod	etched Ni rod	etched Ni foam	reduced Ni foam
R_Ω/Ω $E = -0.20$ V	7.5 ± 0.1	7.2 ± 0.1	3.4 ± 0.2	4.3 ± 0.2
R_Ω/Ω $E = -0.25$ V	7.4 ± 0.1	7.2 ± 0.1	3.4 ± 0.2	4.3 ± 0.2
Y_o/Ω^{-1} $E = -0.20$ V	$(9.83 \pm 2.10) \times 10^{-6}$	$(1.62 \pm 0.19) \times 10^{-5}$	$(3.11 \pm 0.39) \times 10^{-4}$	$(2.29 \pm 0.25) \times 10^{-4}$
Y_o/Ω^{-1} $E = -0.25$ V	$(9.18 \pm 2.10) \times 10^{-6}$	$(1.43 \pm 0.27) \times 10^{-5}$	$(3.19 \pm 0.19) \times 10^{-4}$	$(2.32 \pm 0.19) \times 10^{-4}$
n $E = -0.20$ V	0.97 ± 0.01	0.96 ± 0.01	0.90 ± 0.03	0.88 ± 0.03
n $E = -0.25$ V	0.97 ± 0.01	0.97 ± 0.01	0.88 ± 0.04	0.87 ± 0.03
R_{ct}/Ω $E = -0.20$ V	807 ± 37	507 ± 24	43 ± 3	94 ± 5
R_{ct}/Ω $E = -0.25$ V	211 ± 11	157 ± 12	18 ± 3	33 ± 2
C_{tot}/μF $E = -0.20$ V	7.47 ± 1.80	10.6 ± 1.8	133 ± 36	75 ± 12
C_{tot}/μF $E = -0.25$ V	7.32 ± 1.80	10.6 ± 2.8	121 ± 31	74 ± 12

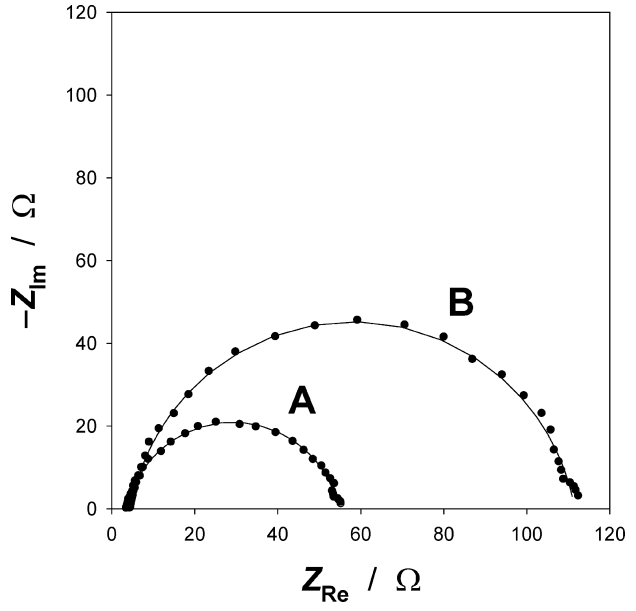

Figure 10. Nyquist plots, Z_{Im} vs Z_{Re}, at $E = -0.225$ V in 0.5 M aqueous KOH solution at $T = 298$ K for the (A) "etched-passivated" and (B) "reduced-passivated" Ni foams. Points represent experimental results and solid lines represent fits obtained using the equivalent circuit shown in Figure 9.

respectively. Finally, we determined $c_{ox,s}$ for the two Ni foams by dividing the C_{ox} values by the respective A_{ecsa} values, and determined that $c_{ox,s}$ equals 7.96 ± 1.17 and 8.03 ± 1.34 μF cm^{-2} for the "etched-passivated" and "reduced-passivated" Ni foams, respectively.

Combination of eqs 4 and 5 results in the following formula that expresses A_{ecsa} as a function of C_{tot}, r, $c_{m,s}$ and $c_{ox,s}$:

$$A_{ecsa} = \frac{C_{tot}}{c_{m,s} + r c_{ox,s}}(1 + r) \quad (9)$$

We used eq 9, the known value of $c_{m,s}$, the experimentally determined value of $c_{ox,s}$, the value of r determined through XPS measurements, and an average of the experimentally determined values of C_{tot} at $E = -0.20$ and -0.25 V vs RHE (Table 2) to calculate A_{ecsa} of the "etched" and "reduced" Ni foams and found that it is 7.23 ± 2.40 and 4.80 ± 0.69 cm^2, respectively. Finally, we were able to calculated A_s and found that it is 241 ± 80 and 160 ± 23 cm g^{-1} for the "etched" and "reduced" Ni foams, respectively.

Comparison of Electrochemically Active and Specific Surface Area Values. In the course of research, we applied complementary approaches, namely combined CV and XPS experiments and CV, XPS and EIS measurements, to determine A_{ecsa} of Ni rods and A_s of Ni foams and summarize the results in Table 3. Because the approach employing EIS measurements still relies on CV and XPS data, it improves the accuracy of A_{ecsa} determination but is not a completely independent method. Their analysis reveals that the A_{ecsa} and A_s values correlate well and that their difference is 13% or smaller in the case of Ni rods and 7% or smaller in the case of Ni foams. While the evaluation of A_{ecsa} and A_s of Pt and Au electrode materials is straightforward and yields fairly accurate values,[54,60,61] the evaluation of A_{ecsa} and A_s of non-noble metal electrode materials having extended surface areas is difficult and often results in very large experimental uncertainties. The good agreement observed in the evaluation of A_{ecsa} and A_s of Ni rods and foams using the complementary methods indicates that one approach alone could be successfully employed to determine A_{ecsa} and A_s of a new type of large surface area Ni material. Although we studied the applicability of these methods only to Ni electrode materials, it is apparent that the same or similar approaches could be adapted to other non-noble electrode materials (e.g., Fe or Co). We also observe that the etching solution 1 applied for a short period of time can be successfully employed to remove native oxides/hydroxides that cover Ni materials without causing any damage to an extended three-dimensional structure.

Table 3. Comparison of A_{ecsa} and A_s Values for Ni Materials Determined Using CV and XPS or EIS.

electrode material and its A_{ecsa} or A_s	CV-XPS analysis	CV-XPS-EIS analysis	difference in A_{ecsa} or A_s (%)
polished Ni rod A_{ecsa} (cm^2)	0.40 ± 0.13	0.37 ± 0.09	8
etched Ni rod A_{ecsa} (cm^2)	0.61 ± 0.15	0.53 ± 0.14	13
etched Ni foam A_s (cm^2 g^{-1})	227 ± 74	241 ± 80	6
reduced Ni foam A_s (cm^2 g^{-1})	149 ± 48	160 ± 23	7

CONCLUSIONS

In summary, our results demonstrate that a comprehensive analysis of Ni foams can be performed by using surface science and electrochemical techniques. Such determined properties can be related to bulk Ni materials and differences arising from the presence of extended surface can be identified and quantified. The surfaces of Ni foams exposed to moist air for extended periods of time revealed both passivated and metallic sections, as proven by XPS and CV measurements. These results point to remarkable stability of Ni foams despite sintering in an oxidizing environment at high temperatures and prolonged exposure to moist air. Careful application of an etching solution facilitated the removal of a native oxide/hydroxide layer from Ni foam surfaces without causing any damage to their three-dimensional structure. The chemical etching increased the electrochemically active and specific surface areas of Ni foams. A native oxide/hydroxide layer residing on Ni foams was reduced thermally in an H_2(g) atmosphere. However, such prepared nonoxidized Ni foam electrodes revealed lower electrocatalytic activity toward surface oxidation than nonoxidized Ni foams produced by chemical etching. Complementary but not completely independent methods were employed to determine in situ the electrochemically active and specific surface areas of Ni foams; the employment of electrochemical impedance spectroscopy improves the accuracy of A_{ecsa} determination through CV and XPS measurements. Consequently, CV and XPS or CV, XPS, and EIS experiments can be successfully applied to determine the electrochemically active and specific surface areas of Ni materials having an extended area and irregular three-dimensional structure. Nickel foams and meshes are used as current collectors and active mass supports in rechargeable batteries. A native oxide/hydroxide layer, which resides on the surface of Ni foam or Ni mesh, gives rise to an overpotential that reduces the battery's power output. Because the chemical etching can remove the native oxide/hydroxide without introducing any structural change, this surface treatment

could be successfully employed to improve the power output of rechargeable batteries.

AUTHOR INFORMATION

Corresponding Author

*E-mail: gregory.jerkiewicz@chem.queensu.ca. Tel.: (613) 533-6413.

Present Address

[†]Permanent address the Faculty of Chemistry, Warsaw University, Ul. Pasteura 1, 02−093 Warsaw, Poland

Notes

The authors declare no competing financial interest.

ACKNOWLEDGMENTS

We gratefully acknowledge financial support towards this project from the NSERC of Canada (Discovery Grant, Research Tools and Instruments Grants, Strategic Research Project) and the Emerging Materials Knowledge of the Materials and Manufacturing Ontario. We gratefully acknowledge collaboration with VALE (formerly Vale-Inco) and discussions with Drs. V. Paserin and Q. Yang. M.G. acknowledges a leave of absence from Warsaw University. M.A. thanks Kuwait University for a graduate fellowship.

REFERENCES

(1) Czerwiński, A.; Dmochowska, M.; Grdeń, M.; Kopczyk, M.; Wójcik, G.; Młynarek, G.; Kołata, J.; Skowroński, J. M. *J. Power Sources* **1999**, *77*, 28.

(2) Czerwiński, A.; Żelazowska, M. *J. Power Sources* **1997**, *64*, 29.

(3) Rogulski, Z.; Lewdorowicz, W.; Tokarz, W.; Czerwiński, A. *Pol. J. Chem.* **2004**, *78*, 1357.

(4) Wang, J.; Dewald, H. D. *Talanta* **1982**, *29*, 453.

(5) Frenzel, W.; Schulze, G. *Analyst* **1987**, *112*, 133.

(6) Langlois, S.; Coeuret, F. *J. Appl. Electrochem.* **1989**, *19*, 51.

(7) Kummer, M.; Kirchhoff, J. R. *Anal. Chem.* **1993**, *65*, 3720.

(8) Desilvestro, J.; Haas, O. *J. Electrochem. Soc.* **1990**, *137*, 5C.

(9) Hitz, C.; Lasia, A. *J. Electroanal. Chem.* **2001**, *500*, 213.

(10) Popczyk, M.; Budniok, A.; Lasia, A. *Int. J. Hydrogen Energy* **2005**, *30*, 265.

(11) Nakaoka, K.; Ueyama, J.; Ogura, K. *J. Electroanal. Chem.* **2004**, *571*, 93.

(12) Dicks, A. L. *Curr. Opin. Solid State Mater. Sci.* **2004**, *8*, 379.

(13) Kleperis, J; Wójcik, G.; Czerwiński, A.; Skowroński, J.; Kopczyk, M.; Bełtowska-Brzezinska, M. *J. Solid State Electrochem.* **2001**, *5*, 229.

(14) Arico, A. S.; Bruce, P.; Scrosati, B.; Tarascon, J. M.; Van Schalkwijk, W. *Nat. Mater.* **2005**, *4*, 366.

(15) Ganesh, V.; Pitchumani, S.; Lakshminarayanan, V. *J. Power Sources* **2006**, *158*, 1523.

(16) Liu, K. C.; Anderson, M. A. *J. Electrochem. Soc.* **1996**, *143*, 124.

(17) Liu, P. S.; Liang, K. M. *J. Mater. Sci.* **2001**, *36*, 5059.

(18) Paserin, V.; Marcuson, S.; Shu, J.; Wilkinson, D. S. *Adv. Eng. Mater.* **2004**, *6*, 454.

(19) Olurin, O. B.; Wilkinson, D. S.; Weatherly, G. C.; Paserin, V.; Shu, J. *Compos. Sci. Technol.* **2003**, *63*, 2317.

(20) Queheillalt, D. T.; Hass, D. D.; Sypeck, D. J.; Wadley, H. N. G. *J. Mater. Res.* **2001**, *16*, 1028.

(21) Dillard, T.; N'guyen, F.; Maire, E.; Salvo, L.; Forest, S.; Bienvenu, Y.; Bartout, J. D.; Croset, M.; Dendievel, R.; Cloetens, P. *Philos. Mag.* **2005**, *85*, 2147.

(22) Carpenter, G. J. C.; Wronski, Z. S.; Phaneuf, M. W. *Mater. Sci. Technol.* **2004**, *20*, 1421.

(23) Brown, I. J.; Sotiropoulos, S. *J. Appl. Electrochem.* **2001**, *31*, 1203.

(24) Liu, P. S.; Liang, K. M. *Mater. Sci. Technol.* **2000**, *16*, 575.

(25) Campbell, R.; Bakker, M. G.; Treiner, C.; Chevalet, J. *J. Porous Mater.* **2004**, *11*, 63.

(26) He, K. X.; Wu, Q. F.; Zhang, X. G.; Wang, X. L. *J. Electrochem. Soc.* **2006**, *153*, A1568.

(27) Skowroński, J. M.; Ważny, A. *J. Solid State Electrochem.* **2005**, *9*, 890.

(28) He, H.; Liu, H.; Liu, F.; Zhou, K. *Mater. Lett.* **2005**, *59*, 3968.

(29) Boukamp, B. A. *Solid State Ionics* **1986**, *20*, 31.

(30) Machado, S. A. S.; Avaca, L. A. *Electrochim. Acta* **1994**, *39*, 1385.

(31) Graedel, T. E.; Leygraf, C. *J. Electrochem. Soc.* **2000**, *147*, 1010.

(32) Medway, S. L.; Lucas, C. A.; Kowal, A.; Nichols, R. J.; Johnson, D. *J. Electroanal. Chem.* **2006**, *587*, 172.

(33) de Souza, L. M. M.; Kong, F. P.; McLarnon, F. R.; Muller, R. H. *Electrochim. Acta* **1997**, *42*, 1253.

(34) Simon, D.; Phu, S. U.; Perrin, C. *J. Chim. Phys.* **1995**, *92*, 1179.

(35) Grosvenor, A. P.; Biesinger, M. C.; Smart, R.St.C.; McIntyre, N. S. *Surf. Sci.* **2006**, *600*, 1771.

(36) Roberts, M. W.; Smart, R.St.C. *J. Chem. Soc., Faraday Trans. I* **1984**, *80*, 2957.

(37) van Veenendaal, M. A.; Sawatzky, G. A. *Phys. Rev. Lett.* **1993**, *70*, 2459.

(38) Gencheva, P.; Tzvetkoff, T.; Bojinov, M. *Appl. Surf. Sci.* **2005**, *241*, 459.

(39) Wruck, D. A.; Rubin, M. *J. Electrochem. Soc.* **1993**, *140*, 1097.

(40) Siconolfi, D. J.; Frankenthal, R. P. *J. Electrochem. Soc.* **1989**, *136*, 2475.

(41) Furstenau, R. P.; McDougall, G.; Langell, M. A. *Surf. Sci.* **1985**, *150*, 55.

(42) Hillebrecht, F. U.; Fuggle, J. C.; Bennett, P. A.; Zołnierek, Z.; Freiburg, C. *Phys. Rev. B* **1983**, *27*, 2179.

(43) Biesinger, M. C.; Payne, B. P.; Grosvenor, A. P.; Lau, L. W. M.; Gerson, A. R.; Smart, R.St.C. *Appl. Surf. Sci.* **2011**, *257*, 2717.

(44) Grdeń, M.; Klimek, K. *J. Electroanal. Chem.* **2005**, *581*, 122.

(45) Dmochowska, M.; Czerwiński, A. *J. Solid State Electrochem.* **1998**, *2*, 16.

(46) Hahn, F.; Floner, D.; Beden, B.; Lamy, C. *Electrochim. Acta* **1987**, *32*, 1631.

(47) Seghiouer, A.; Chevalet, J.; Barhoun, A.; Lantelme, F. *J. Electroanal. Chem.* **1998**, *442*, 113.

(48) Seyeux, A.; Maurice, V.; Klein, L. H.; Marcus, P. *J. Solid State Electrochem.* **2005**, *9*, 337.

(49) Alsabet, M.; Grden, M.; Jerkiewicz, G. *Electrocatalysis* **2011**, *2*, 317.

(50) Ganesh, V.; Lakshminarayanan, V. *Electrochim. Acta* **2004**, *49*, 3561.

(51) Conway, B. E.; Bai, L. *J. Chem. Soc., Faraday Trans. 1* **1985**, *81*, 1841.

(52) Zoltowski, P. *Electrochim. Acta* **1993**, *38*, 2129.

(53) Lasia, A.; Rami, A. *J. Electroanal. Chem.* **1990**, *294*, 123.

(54) Trasatti, S.; Petrii, O. A. *Pure Appl. Chem.* **1991**, *63*, 711.

(55) Rausch, S.; Wendt, H. *J. Electrochem. Soc.* **1996**, *143*, 2852.

(56) Krstajić, N.; Popović, M.; Grgur, B.; Vojnović, M.; Šepa, D. *J. Electroanal. Chem.* **2001**, *512*, 16.

(57) Brug, G. J.; Van Den Eeden, A. L. G.; Sluyters-Rehbach, M.; Sluyters, J. H. *J. Electroanal. Chem.* **1984**, *176*, 275.

(58) Sluyters-Rehbach, M. *Pure Appl. Chem.* **1994**, *66*, 1831.

(59) Qian, Y.; Conway, B. E.; Jerkiewicz, G. *Int. J. Hydrogen Energy* **2000**, *25*, 539.

(60) Rand, D. A. J.; Woods, R. *J. Electroanal. Chem.* **1972**, *36*, 57.

(61) Burshtein, R. K.; Tarasevich, M. R.; Vilinskaya, V. S. *Elektrokhimiya* **1967**, *3*, 349.

(62) Weininger, J. L.; Breiter, M. W. *J. Electrochem. Soc.* **1963**, *110*, 484.

(63) Weininger, J. L.; Breiter, M. W. *J. Electrochem. Soc.* **1964**, *111*, 707.

(64) Yau, S. L.; Fan, F. R. F.; Moffat, T. P.; Bard, A. J. *J. Phys. Chem.* **1994**, *98*, 5493.

(65) Parthasaradhy, N. V. *Practical Electroplating Handbook*; Prentice Hall: Englewood Cliffs, NJ, 1989.